Synthesis, Microwave Electromagnetic, and Microwave Absorption Properties of Twin Carbon Nanocoils

ARTICLE *in* THE JOURNAL OF PHYSICAL CHEMISTRY C · DECEMBER 2008

Impact Factor: 4.77 · DOI: 10.1021/jp808087n

7 AUTHORS, INCLUDING:

Chak Tong Au
Hong Kong Baptist University
410 PUBLICATIONS **7,760** CITATIONS
SEE PROFILE

yi Yang
Nanjing University
24 PUBLICATIONS **565** CITATIONS
SEE PROFILE

Mangui Han
University of Electronic Science and Techn…
77 PUBLICATIONS **803** CITATIONS
SEE PROFILE

Youwei Du
Dalian Maritime University
317 PUBLICATIONS **4,091** CITATIONS
SEE PROFILE

THE JOURNAL OF PHYSICAL CHEMISTRY C

Article

Synthesis, Microwave Electromagnetic, and Microwave Absorption Properties of Twin Carbon Nanocoils

Nujiang Tang, Wei Zhong, Chaktong Au, Yi Yang, Mangui Han, Kuanjiuh Lin, and Youwei Du

J. Phys. Chem. C, **2008**, 112 (49), 19316-19323 • Publication Date (Web): 13 November 2008

Synthesis, Microwave Electromagnetic, and Microwave Absorption Properties of Twin Carbon Nanocoils

Nujiang Tang,*,† Wei Zhong,† Chaktong Au,‡ Yi Yang,*,† Mangui Han,§ Kuanjiuh Lin,|| and Youwei Du†

Nanjing National Laboratory of Microstructures, Nanjing University, Nanjing 210093, P. R. China, Chemistry Department and Center for Surface Analysis and Research, Hong Kong Baptist University, Hong Kong, P. R. China, State Key Laboratory of Electronic Thin Films and Integrated Devices, University of Electronic Science and Technology of China, Chengdu 610054, P. R. China, and Department of Chemistry and Center of Nanoscience and Nanotechnology, National Chung-Hsing University, Taichung 402, Taiwan, Republic of China

Received: September 11, 2008; Revised Manuscript Received: October 26, 2008

Twin carbon nanocoils (T-CNCs) were synthesized by means of acetylene decomposition over nickel nanoparticles. From the TEM image, one can see the growth of carbon nanocoils from the opposite sides of a nickel nanodisc, making an interangle of 180°. We examined the microwave electromagnetic (EM) and microwave-absorbing properties of the as-prepared and annealed (1400 °C in Ar) T-CNCs systematically. A composite containing the as-prepared T-CNCs (15 wt %) and paraffin exhibited strong microwave absorption in a frequency range of 2 to 18 GHz. Over an absorber of double-layered composite (2.5 and 3.5 mm thickness), an absorption bandwidth of ca. 10 GHz corresponding to reflection loss below −10 dB can be obtained. We found that the magnetic parameters of the composite are low and suggest that the good absorption properties of T-CNCs should be attributed to dielectric rather than magnetic loss. It was observed that the as-prepared T-CNCs are superior to the annealed T-CNCs in microwave absorption ability, and such a phenomenon is interpreted in terms of the defect and graphitic nature of the materials. We also demonstrated that the complex permittivity and electric conductivity of T-CNCs can be controlled via annealling of T-CNCs at high temperature.

Introduction

Microwave-absorbing materials (MAMs) have wide commercial and military applications.[1] Besides being applied in electronic devices and systems of wireless antenna and cellular phones, they are used as radar absorbents and shielding substances against electromagnetic (EM) interference. Traditionally, MAMs are particles of magnetic metals or alloys, and because of high specific gravity and formulation difficulty, they are restricted in application. It is hence desirable to have MAMs that are lightweight, structurally sound, and flexible and show good microwave-absorbing ability in a wide frequency range. In terms of these criteria, one-dimensional carbon-based substances appear to be good candidates. Scientists have studied the morphology and physical nature of carbon microcoils (CMCs) and carbon nanocoils (CNCs), and potential applications of these materials have been suggested in relation to their chiral structures and unique physical properties.[2−11] Indeed, the electrical and mechanical properties of the materials have been investigated for nanoengineering.[3−6,10,12] Also, field emission[13] and chemical[14] and thermal[15] properties of the materials have been studied for various kinds of applications. It has been widely reported that the materials are good for EM wave absorption.[16]

Generally speaking, carbon coils can be prepared via high-temperature (>700 °C) catalytic decomposition of organic vapors such as acetylene or benzene over powder of a transition metal (e.g., Ni) or its alloys. Motojima et al. synthesized double-helix CMCs of ca. 0° interangle via a high-temperature route. They reported that the Ni particles are often located at the tips. The as-grown CMCs were largely amorphous, and annealing at 2500 °C was required for better graphitization.[17] The authors also found that paired straight fibers rather than coils were generated below 700 °C, and they attributed the result to change of anisotropy during carbon deposition at low temperatures.[17] Recently, twin carbon nanosheets were synthesized by chemical vapor deposition using acetylene as the source gas and Cu nanowires as catalysts at 250 °C. The nanosheets follow the alignment of the original Cu nanowire arrays, and each Cu nanowire always initiates the symmetric growth of twin nanosheets in opposite directions.[18] We reported previously the low-temperature synthesis of crystalline helical carbon nanofibers (HCNFs),[19] helical carbon nanotubes (HCNTs),[20] and plaite-like CNCs.[21] To the best of our knowledge, no work has been done on synthesis of crystalline twin carbon nanocoils (T-CNCs) with the two coils growing opposite to each other (interangle = 180°). Herein, we report the synthesis of such a kind of material via decomposition of acetylene at 415 °C over Ni nanoparticles derived from a combined method of sol−gel fabrication and hydrogen reduction. The magnetic, microwave EM, and microwave-absorbing properties of the T-CNC materials were examined in detail. We found that the T-CNC material is superior to CMCs[16] and plaite-like CNCs[21] in microwave absorption ability.

* Corresponding author. E-mail: tangnujiang@nju.edu.cn.
† Nanjing University.
‡ Hong Kong Baptist University.
§ University of Electronic Science and Technology of China.
|| National Chung-Hsing University.

10.1021/jp808087n CCC: $40.75
Published on Web 11/13/2008

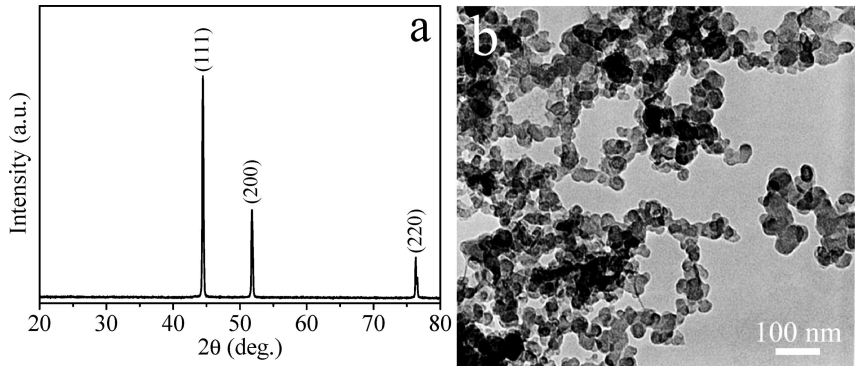

Figure 1. (a) XRD pattern and (b) TEM image of catalyst.

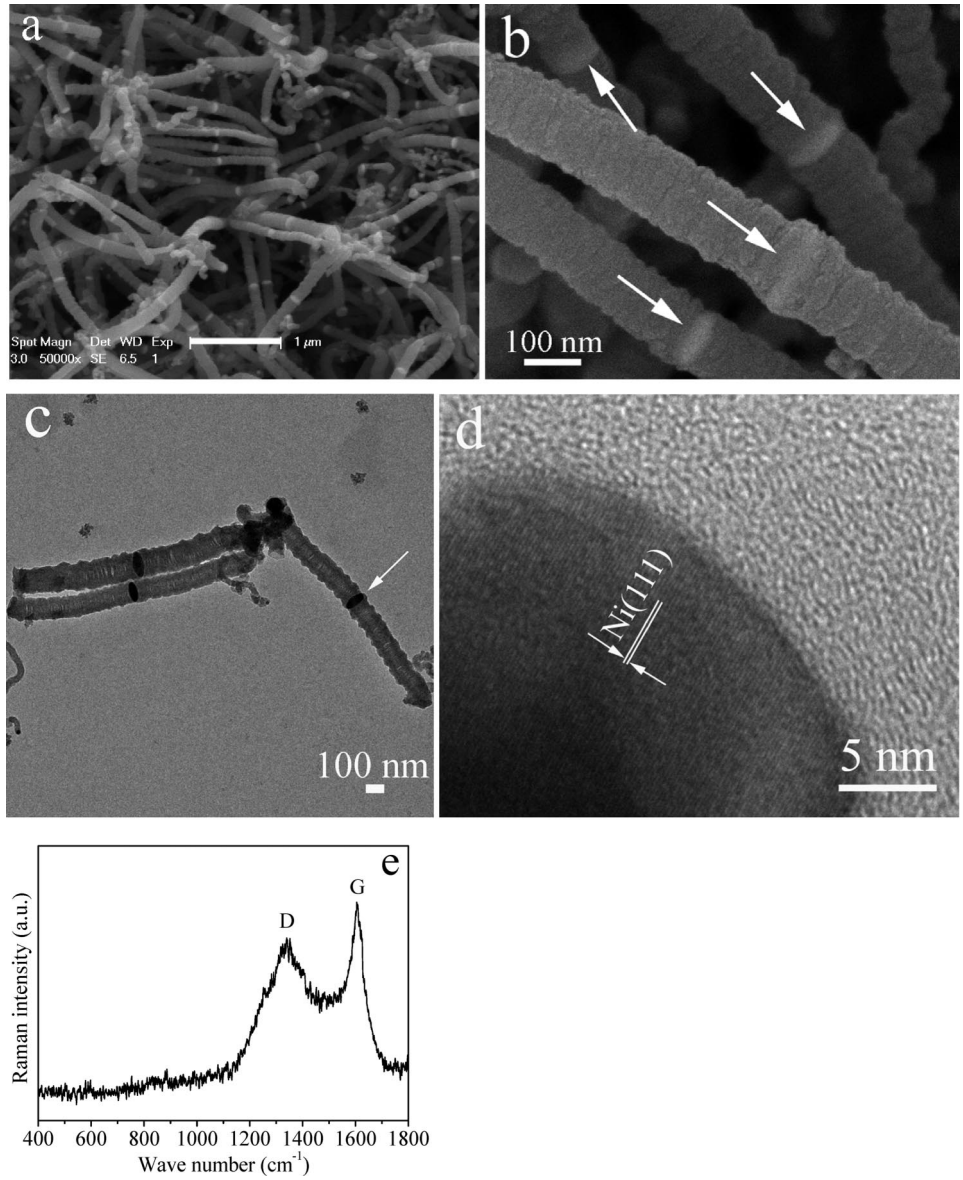

Figure 2. Structure of T-CNCs generated over 51 mg of NiO nanoparticles at 415 °C. (a) and (b) Typical FE-SEM images with arrows indicating Ni nanodiscs; (c) TEM image; (d) HR-TEM image of spot indicated by an arrow in (c); and (e) Raman spectrum.

Experimental Section

In brief, 51 mg of NiO powder was spread on a ceramic plate and placed inside a quartz tube (4.39 cm outer diameter and 35 cm length). With the quartz tube located in a stainless steel tube of 5.2 cm inner diameter (equipped with temperature and gas-flow controls), the NiO powder was reduced in H_2 at 375 °C for 1 h. Then decomposition of acetylene was conducted at 415 °C for 0.5 h at atmospheric pressure over the nickel nanoparticles. With cooling to room temperature (RT), approximately 0.364 g of as-prepared T-CNCs could be collected. To obtain

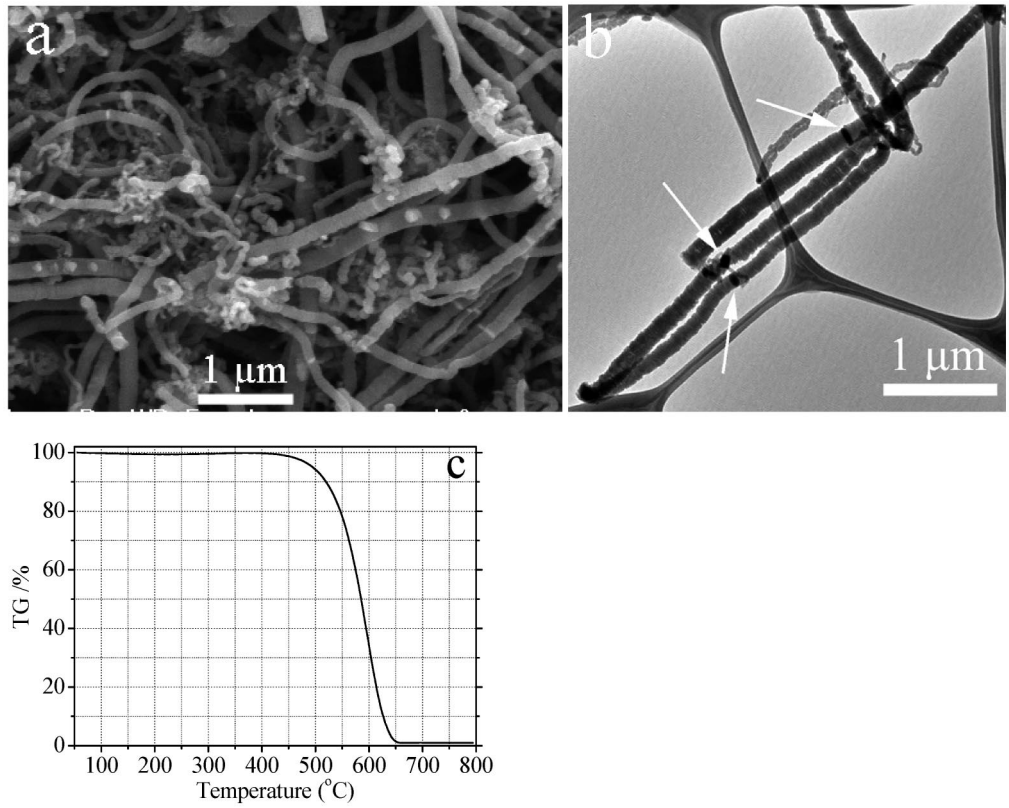

Figure 3. (a) Typical FE-SEM, (b) TEM image (arrows indicating Ni nanodiscs), and (c) thermogravimetric (TG) curve of T-CNCs generated at 425 °C.

the "annealed" T-CNCs, the as-prepared T-CNCs obtained at a decomposition temperature of 425 °C were annealed at 1400 °C in Ar for 6 h and then cooled to RT.

The phases of metallic nickel and nickel oxides were determined by X-ray diffraction (XRD) with Cu Kα radiation (model D/Max-RA, Rigaku, Japan) at 5 °C. Raman spectroscopic investigation of T-CNC samples was performed using a Jobin-Yvon LABRAM HR800 instrument with 514.5 nm Ar laser excitation. Thermoanalysis was carried out on a PERKIN ELMER TGA7 Series Thermal Analysis system under the conditions of 3.9 mg of sample heated in air at a rate of 5 °C/min. The morphologies of CNCs samples were examined by transmission electron microscopy (TEM) (model JEM-2000EX, Japan), high-resolution TEM (HR-TEM) (model JEOL-2010, Japan), and field emission scanning electron microscopy (FE-SEM) (model JSM-6700F, Japan) with the equipment operated at an accelerating voltage of 120, 200, and 5 kV, respectively. For TEM analysis, the powder samples were dispersed in ethanol, agitated in an ultrasonic bath, and finally deposited on a copper grid that was coated with a carbon film. The magnetic properties of samples were measured by a SQUID magnetometer (Quantum Design MPMS-XL, USA) equipped with a superconducting magnet capable of producing fields of up to 70 kOe. For microwave measurement, a composite sample containing T-CNCs (with paraffin being the binder matrix) was pressed into a ring of 7 mm outer and 3 mm inner diameter. The complex permeability μ ($\mu = \mu' - j\mu''$) and permittivity ε ($\varepsilon = \varepsilon' - j\varepsilon''$) were measured using an Agilent PNA E8363B network analyzer in the frequency range of 2 to 18 GHz.

Results and Discussion

Microstructure of As-Prepared T-CNCs. The powder XRD pattern of nickel catalyst (which was reduced in H_2 at 375 °C for 1 h) measured at 5 °C is presented in Figure 1a. We detect no sign of nickel oxide and ascribe the diffraction peaks at ca. 44.48°, 51.82°, and 76.36° to Ni of fcc structure. The result indicates that nickel oxide has been reduced to metallic nickel during the reduction process. The nickel particles are spherical and/or quasi-spherical in shape, exhibiting a relatively uniform grain size of 30 nm as revealed in the TEM investigation (Figure 1b).

Figures 2a−c show the FE-SEM and TEM images of as-prepared T-CNCs. The twist and entanglement of CNCs suggest disorder and distortion of material. The T-CNCs have a novel silkworm structure, showing tight coils of very short coil pitches. A closer examination reveals that: (1) there are two CNCs of similar diameter and length (ca. 110 and 750 nm, respectively) grown on opposite sides of an elliptical nickel particle, exhibiting an interangle of 180°; (2) the diameter of coils is roughly the same as that of the nickel nanodisc on which the coils grow; (3) the coils are composed of bundles of nanofibers of ca. 10 nm diameter (Figure 2c), suggesting a much larger aspect ratio. The HR-TEM image (Figure 2d) shows that the Ni nanodisc is single crystalline, and the growth direction of CNCs is vertical to the normal of the (111) plane. The structure of T-CNCs is different from that of CMCs reported before where the Ni particles are often located at the tips of coils, and the pair of coils shows an interangle of about 0°.[17] In the cases of HCNFs[19] and HCNTs[20] grown on Fe nanoparticles, an interangle θ of about 35°, 70°, or 130° was observed. The structure of T-CNCs is also different from that of plait-like CNCs where two CNCs of different handiness form an interangle of 0°.[21] The difference in fabrication procedure is that in the case of plait-like CNCs the NiO powder was spread on a ceramic plate which was placed inside a quartz reaction tube (diameter: 4.39 cm; length: 45 cm),[21] whereas in the case of T-CNCs, the quartz reaction tube

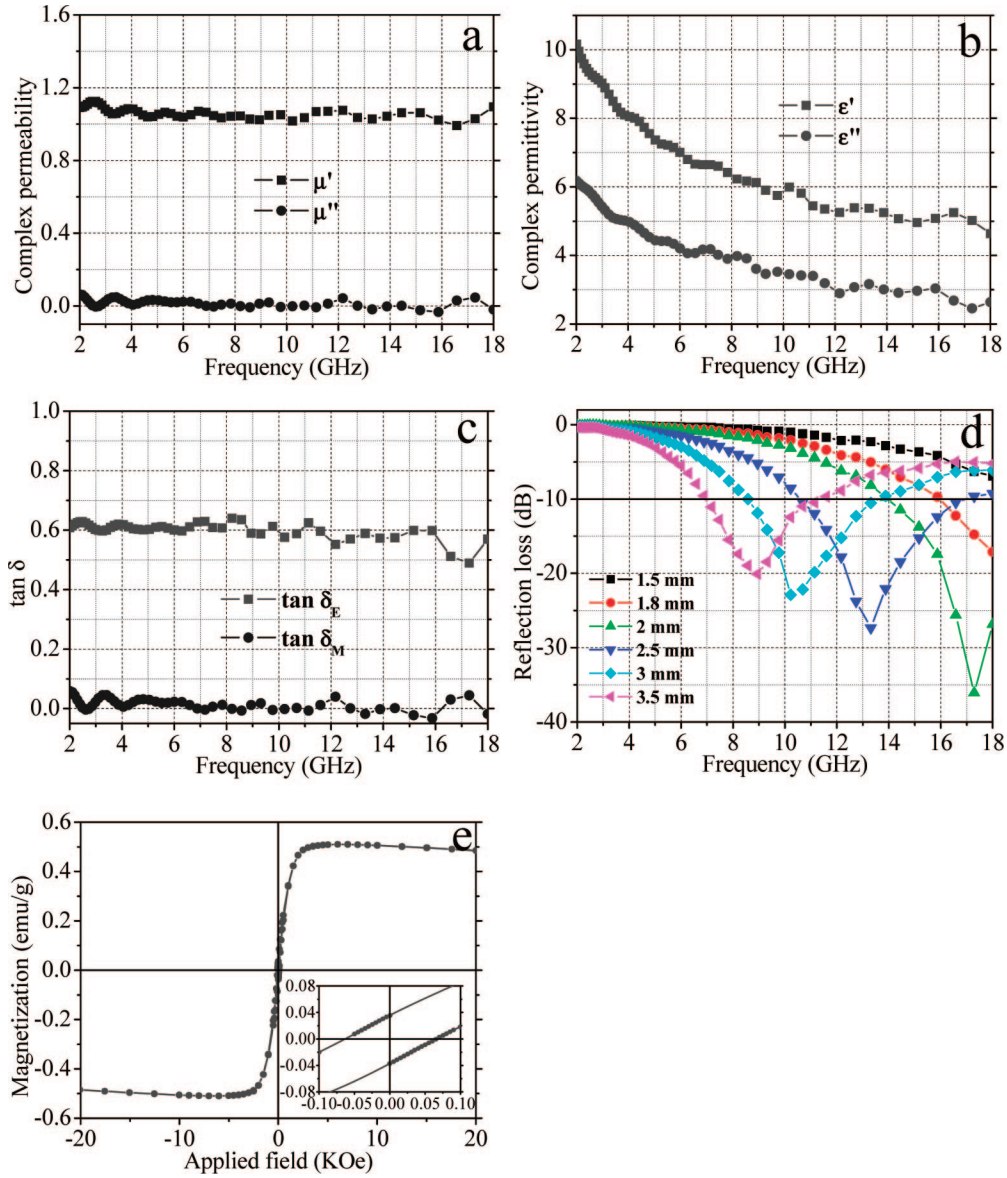

Figure 4. (a) Permeability spectra, (b) permittivity spectra, (c) loss tangent spectra, and (d) reflection loss of the composite sample containing 15 wt % of as-prepared T-CNCs (obtained at 425 °C) measured in the frequency range of 2 to 18 GHz. (e) Typical magnetization curves of as-prepared T-CNCs measured at 300 K by the SQUID magnetometer (maximum applied field was 2 T). Inset is the enlarged part of magnetization curves close to the origin.

was placed in a stainless steel tube of 5.2 cm inner diameter (see Experimental Section). It is apparent that the growth mechanism of carbon nanomaterials is complex and subject to subtle changes of reaction conditions.

The elliptical shape of the Ni nanodisc (110 nm in diameter and 45 nm in thickness, Figures 2b and c) is significantly different from the spherical or quasi-spherical shape of Ni particles (size ca. 30 nm) observed in Figure 1b. It is obvious that under the adopted reaction conditions the nickel nanoparticles adjusted themselves to a discal shape that favors T-CNC growth. The two surfaces of the nanodisc serve as a base for the growth of nanocoils. The Raman spectrum of T-CNCs shows two peaks, one at 1340.2 cm^{-1} and the other at 1604.6 cm^{-1} (Figure 2e). It is known in Raman studies that a peak at 1580 cm^{-1} (called G-band) is characteristic of a crystalline graphite, while a peak at 1350 cm^{-1} (called D-band) is due to disorder of carbon materials.[22] It is apparent that the T-CNC material is graphitic and contain defects.

Effect of Decomposition Temperature. With a change of decomposition temperature from 415 to 425 °C (other conditions unchanged), longer T-CNCs of larger diameter (ca. 160 nm) were obtained (Figures 3a and b). Again the coils are composed of small nanocoils of very small diameter (Figure 3b). Using 51 mg of NiO powder as the catalyst precursor, we obtained 2.41 g of product in a run of 0.5 h. As compared to a yield of 0.364 g at 415 °C (see Experimental), there is a significant increase in T-CNC yield. In other words, the yield of T-CNCs is temperature dependent, and the decomposing temperature of acetylene has a profound influence on the yield of T-CNCs. In terms of carbon to nickel weight ratio, the T-CNC yield is ca. 6013.67%, and Ni content in as-prepared T-CNCs is no more than 1.66 wt %; in other words, purity of T-CNCs is up to 98.34 wt %. The quantitative data were confirmed by thermogravimetric analysis (TG). The ca. 99% weight loss of as-prepared T-CNCs in the temperature range of 450 ~ 700 °C confirmed the aforementioned percentage of T-CNCs (shown in Figure 3c). The leftover powder of ca. 1 wt % can be attributed to NiO powder. It is worth pointing out that the mass production of high-purity T-CNCs via an easy procedure is a determining factor for wide utilization of the material.

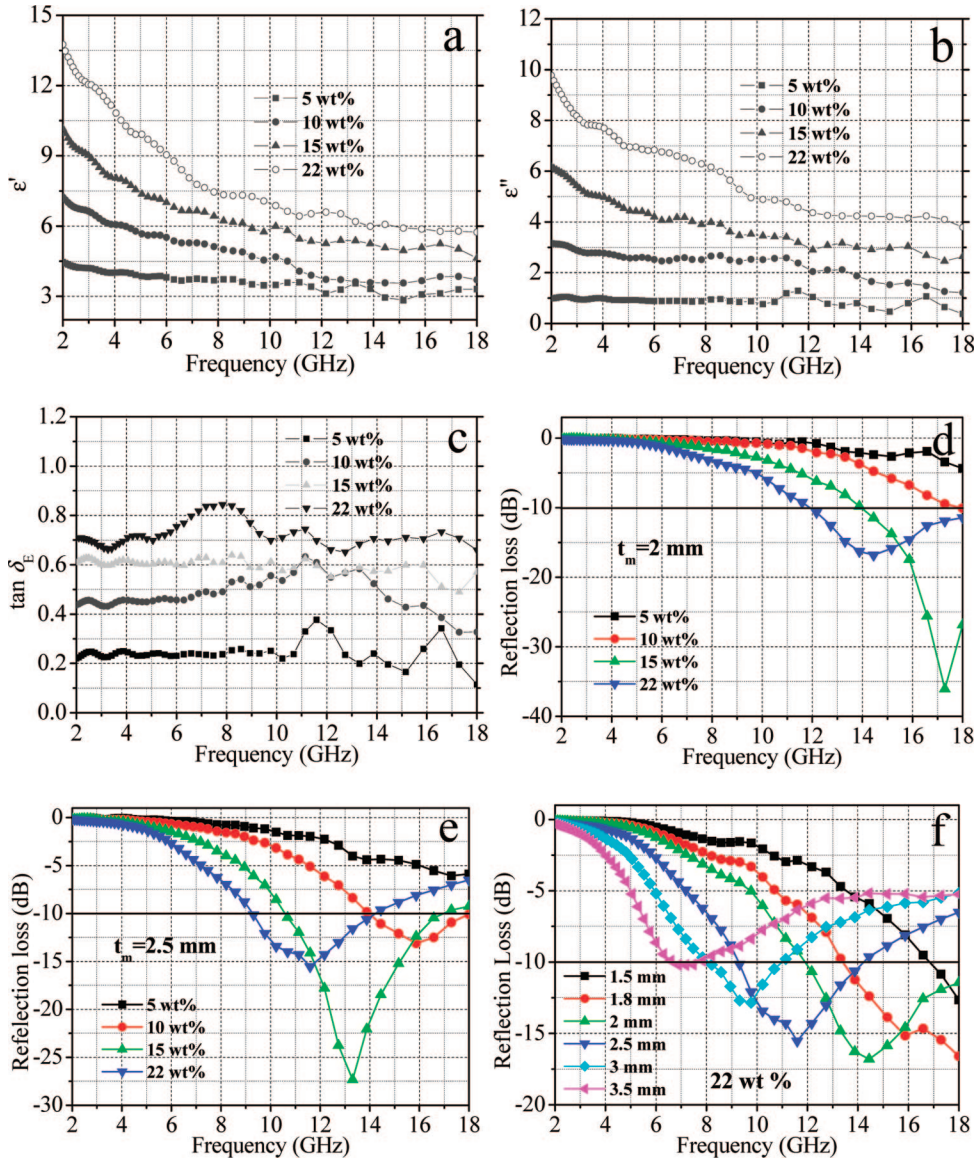

Figure 5. (a−e) Permittivity spectra, tan δ_E spectra, and reflection loss of the composite samples containing paraffin and different content of T-CNCs obtained at decomposing temperature of 425 °C. All of them were measured in the frequency range of 2 to 18 GHz. The t_m in (d) and (e) were 2 mm and 2.5 mm, respectively. (f) Reflection loss of the composite sample containing paraffin and 22 wt % T-CNCs obtained at a decomposing temperature of 425 °C.

Magnetic, Microwave EM, and Microwave-Absorbing Properties of As-Prepared T-CNCs. The microwave EM properties and microwave absorption behavior of a T-CNCs/paraffin composite containing 15 wt % as-prepared T-CNCs were investigated in a frequency range of 2−18 GHz (Figures 4a−d). As shown in Figure 4a of complex permeability, a real part value close to 1.1 and an imaginary part close to 0 can be related to the low content of ferromagnetic Ni nanoparticles in the composite. The low Ni content can also be confirmed by the magnetization curves of as-prepared T-CNCs (Figure 4e). As shown in the M−H curves, saturation magnetization (M_S) and coercivity (H_c) of as-prepared T-CNCs is 0.51 emu g^{-1} (1 emu g^{-1} = 1 Am^2 kg^{-1}) and 63.6 Oe (1 Oe = 79.6 Am^{1-}). On the basis of the fact that the Ni content is ca. 1.66 wt % and the M_S of bulk Ni is ca. 54.39 emu g^{-1} at 300 K, we estimate that the M_S of the T-CNC sample should be around 0.9 emu g^{-1}, which is higher than the 0.51 emu g^{-1} value obtained experimentally. The results reveal the low magnetic parameters of the T-CNCs/paraffin composite. The phenomenon can be related to the nonuniformity in magnetic properties of as-prepared T-CNCs due to the uneven distribution of Ni nanodiscs in the composite samples.

The complex permittivity of composite versus frequency is shown in Figure 4b. One can see a decrease of ε' and ε'' with frequency rise, showing that frequency dispersion is beneficial for impedance matching of incoming microwave. The tangent of dielectric and magnetic loss can be expressed as tan $\delta_E = \varepsilon''/\varepsilon'$ and tan $\delta_M = \mu''/\mu'$, respectively. Figure 4c shows the frequency dependence of tan δ_E/tan δ_M. It is observed that the tan δ_E value is much higher than the tan δ_M value. Since the magnetic parameters of composite are low, one can deduce that the reflection loss is mainly due to dielectric loss. In other words, the absorption of microwave is largely due to dielectric dispersion properties. According to the transmit-line theory[22] and by using the EM parameters of composite samples, one can obtain the reflection loss of microwave (at different composite thicknesses) (Figure 4d). It can be seen that the samples exhibit good ability of microwave absorption. With matching thickness t_m = 2 mm, the maximum reflection loss R_{max} is ca. −36.09 dB at 17.29 GHz. At t_m = 2.5 mm, the

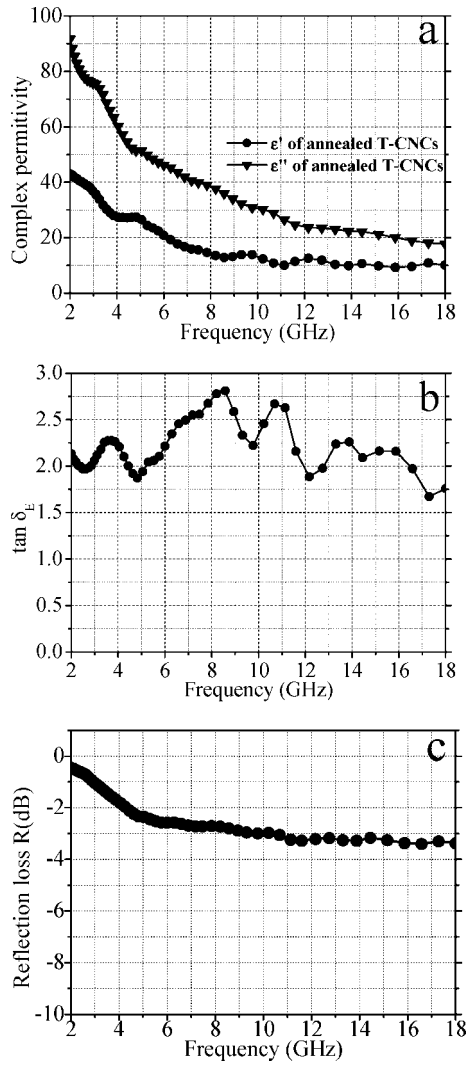

Figure 6. (a−c) Permittivity spectra, tan δ_E spectra, and reflection loss of the composites containing paraffin and 15 wt % of annealed T-CNCs measured in the frequency range of 2 to 18 GHz.

bandwidth corresponding to reflection loss below −10 dB (i.e., over 90% microwave absorption) is higher than 6.43 GHz, whereas at t_m = 3.5 mm, the bandwidth corresponding to reflection loss below −5 dB (i.e., over 70% microwave absorption) is ca. 12.24 GHz. We previously reported that plait-like CNCs obtained in acetylene decomposition at 425 °C exhibits excellent microwave absorbing ability: R_{max} is ca. −20 dB and bandwidth is ca. 4.31 GHz.[21] Clearly, the T-CNC material is superior to plait-like CNCs in microwave absorption. Compared to materials such as single-walled carbon nanotubes (SW-CNTs),[1] multiwalled nanotubes (MW-CNTs),[24] CMCs,[16] iron-filled CNTs,[25] iron-coated carbon fibers,[26] and iron fiber,[27] T-CNCs are also superior. The R_{max} (ca. −36.09 dB) of T-CNCs is even higher than that (−32 dB) of Ni/C nanocapsules reported by Zhang et al.[28] With an increase of composite thickness, there is a shift of reflection loss peak toward lower frequency (Figure 5d). The behavior is important because it reveals that the range of absorption frequency can be tuned via the changing of composite thickness, and broadband absorption can be achieved by means of multilayered absorbent.[29] For example, to reach a reflection loss of below −10 dB, a composite of 2.5 and 3.5 mm thickness has an absorption bandwidth wider than 4 and 6 GHz, respectively. The combination of the two layers could cover a frequency range of 7 to 17 GHz; viz., the bandwidth of the double-layer absorber can reach up to 10 GHz.

The dielectric loss factor tan δ_E and the magnetic loss factor tan δ_M may well explain why the T-CNCs/paraffin composite has such excellent ability of microwave absorption (Figure 4c). One can see that in the frequency range tan δ_E is around 0.6 (with only slight fluctuation), while tan δ_M is below 0.1. The steady dielectric loss proves the balanced property of EM matching. According to the above results, one can recognize that the good ability of T-CNCs for microwave absorption can be attributed to factors such as low ε' and relatively high ε'', excellent frequency dispersion, and steady dielectric loss of the material. In other words, the steady dielectric loss of T-CNCs plays a crucial role in enabling such a broad frequency range (for a reflection loss of below −10 dB).

Over CMCs of about 4 μm coil diameter and 0.5 to 0.8 μm pitch, Shen et al.[16j] detected microwave reflection loss below −10 dB in the frequency range of 10 to 15 GHz, and maximum microwave reflection loss of −18 dB was observed at 12.4 GHz. It has been demonstrated that the chiral parameter value of chiral materials has great impact on microwave absorption.[30] Shen et al. assumed that CMCs with smaller diameter and pitch should have higher chiral parameter value.[16j] With maximum reflection loss of −36.09 dB and bandwidth corresponding to reflection loss below −10 dB up to 6.43 GHz, our T-CNC material is better than the CMCs of Shen et al. in microwave-absorbing ability. Apparently, our results corroborate the assumption made by Shen et al.[16j] The T-CNCs generated at 425 °C over nanoscaled nickel particles have small diameter and very short pitch. Thus, the good microwave absorption performance of T-CNCs can be ascribed to the high chiral parameter value of T-CNCs.

It is known that thickness, reflection loss, and bandwidth are important factors to be considered in the application of radar-absorbing materials. We would like to point out that the T-CNCs content (i.e., 15 wt %) of composite has not been optimized, and a sample of different T-CNCs density might show better performance in microwave absorption. We studied the reflection loss of composite samples of 5.0 to 22 wt % T-CNC content in the frequency range of 2 to 18 GHz. Figures 5a−c show frequency dependence of ε', ε'', and tan δ_E over the composite samples. It can be seen that ε', ε'', and tan δ_E increase with an increase of T-CNC concentration. Figures 5d and e show the absorption properties of T-CNC composites with different T-CNC concentrations. The t_m of Figures 5d and e is 2 and 2.5 mm, respectively; with rise of T-CNCs content, the peak value of reflection loss shifts to lower frequency, and the bandwidth corresponding to reflection loss below −10 dB increases. As shown in Figure 5d of t_m = 2 mm, the peak value reaches a maximum of −36.09 dB at 15 wt % T-CNC content, and maximum absorption decreased to −16.8 dB at T-CNC content of 22 wt % (bandwidth = 4.93 GHz). As illustrated in Figure 5f, the bandwidth corresponding to reflection loss below −5 dB is as high as 13 GHz at a T-CNC content of 22 wt % and t_m = 3.5 mm. It is obvious that one can obtain full-band absorption (below −5 dB, viz. over 70% microwave absorption) covering a frequency range of 2 to 18 GHz by compiling two composite layers of different thicknesses.

Fan et al. pointed out that with an increase of CNT content in composite, the electric field of short-distance resonance multipoles leads to dominance of reflection property rather than adsorption property. They reported that ε increasd with increasing CNT concentration, resulting in a shift of reflectivity peak toward lower frequency.[24c] In other words, it is possible to achieve better microwave absorption by optimizing the T-CNCs content in the 10 to 22 wt % range. The revelation is important

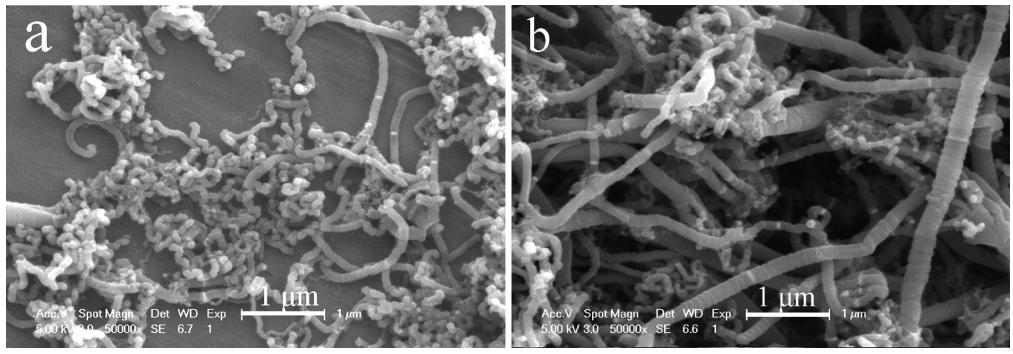

Figure 7. FE-SEM images of CNCs obtained in acetylene decompostion at 425 °C using (a) 0.1 g and (b) 0.15 g of NiO as catalyst precursor.

because it suggests that the range of absorption frequency can be easily tuned by changing the T-CNC content of composite. Thus, wideband absorption could be achieved by compiling T-CNCs/paraffin layers of different T-CNC contents. For example, for reflection loss below −10 dB, composites of 15 and 22 wt % T-CNC content in 2.5 mm thickness have absorbing bandwidths wider than 5 and 6 GHz, respectively. The combination of the two could cover a frequency range of 9 to 17 GHz, indicating that a bandwidth ca. 8 GHz can be obtained in this double-layer absorber. It is commonly known that a thin MAM layer of wideband absorption properties is hard to fabricate based on a single material. In view that the nature of absorption can be easily tuned by variation of T-CNC content and/or composite thickness and further optimization is feasible via proper design of multilayered structure, we believe that the T-CNC material has great potential for wideband microwave absorption. Recently, there are reports showing that the microwave-absorbing ability of CNTs[24a] and CNCs[31] can be enhanced via the doping of foreign magnetic materials. It is likely that the microwave-absorbing ability of T-CNCs can be enhanced with doping of suitable magnetic materials as well.

Microwave EM and Microwave-Absorbing Properties of Annealed T-CNCs. It is known that by raising the graphitization level of CNCs one can enhance electrical conductivity.[32] As mentioned before, good electric conductivity leads to dominance of reflection property rather than absorption property, and a low electrical conductivity is desired for improvement of microwave absorption properties.[24,28] To study the effect of graphitization enhancement, we annealed the as-prepared T-CNCs at 1400 °C in Ar for 6 h and prepared a composite containing 15 wt % annealed T-CNCs in paraffin. The frequency dependence of permittivity measured in the frequency range of 2 to 18 GHz over the composite is shown in Figure 6a. One can see that ε' and ε'' of the composite with annealed T-CNCs are higher than those of the one with as-prepared T-CNCs (shown in Figure 4b), confirming that the electrical conductivity of annealed T-CNCs is higher than that of as-prepared T-CNCs,[24,26,27] plausibly due to the higher degree of graphitization of the former.[32] Figure 6b shows frequency vs tan δ_E over the composite of annealed T-CNC. It is observed that across the frequency tan δ_E is above 1.5 and much higher than that of as-prepared T-CNC composites (shown in Figure 4c), whereas dielectric loss is not as steady as that of the as-prepared T-CNC composites. Figure 6c shows the reflection loss of the annealed T-CNC composite with $t_m = 2$ mm. It is interesting to find that the reflection loss of the annealed T-CNC composite sample is below −3.4 dB. Compared to the as-prepared T-CNC composite, the annealed T-CNC composite shows much lower microwave absorption ability. In other words, the microwave absorption properties of T-CNCs decrease significantly after T-CNCs annealing at high temperature. On the basis of the results, we deduce that the good microwave absorption ability of as-prepared T-CNCs is attributable to the relatively high electric resistivity and steady dielectric loss of the material. It is suggested that the relatively high electric resistivity of as-prepared T-CNCs is a result of poor graphitization and defect presence. In other words, the adoption of the low-temperature (ca. 425 °C) synthesis route is favorable for the fabrication of T-CNCs for microwave absorption.

Effect of Catalyst Amount on T-CNCs Fabrication. We found that the amount of precursor catalyst has a profound influence on the yield of carbon products. If 100 mg of NiO nanoparticles was used, ca. 3.027 g of product was collected in each run, equivalent to a CNC yield of 3751.1%. Compared to a CNC yield of 6013.67% in the case of 51 mg of NiO, there is in fact a decrease. As shown in the FE-SEM image (Figure 7a), there is a dense population of single-helix CNCs. If 150 mg of precursor catalyst was used, the yield in each run under similar conditions was significantly reduced to ca. 2.911 g, and T-CNCs became the major product (Figure 7b). On the basis of the results, we deduce that the rate of acetylene decomposition has a determining effect on T-CNC selectivity and yield. With the adoption of an appropriate amount of catalyst, the rate of acetylene decomposition can be regulated for maximum T-CNC generation. During the growth of HCNTs over Fe nanoparticles, we observed a different scenario in which higher HCNT yield was achieved by increasing the amount of Fe nanoparticles.[20] Nevertheless, the complex permeability, complex permittivity, and microwave absorption properties of the CNCs generated over 100 or 51 mg of NiO nanoparticles are similar. Disregarding the variation in yield, the two kinds of T-CNCs display similar microwave EM and microwave absorption properties.

Conclusions

In summary, we reported the synthesis of novel T-CNCs via a low-temperature (ca. 415 °C) and environmentally friendly route of catalytic decomposition of acetylene over Ni nanoparticles. The yield of as well as selectivity to T-CNCs or single helical CNCs can be controlled by regulating the decomposition temperature and the amount of catalyst. The as-prepared T-CNCs obtained at 425 °C over 51 mg of catalyst precursor display good microwave absorption ability, and wideband absorption is possible when a double-layered absorber made of two composites of different thicknesses or T-CNC contents is used. Thus, we have found a simple and low-cost approach for large-scale fabrication of lightweight T-CNCs for widerband microwave absorption. We also demonstrated that complex permittivity and the electric conductivity of the as-prepared T-CNCs can be enchanced significantly via annealing the

material at 1400 °C. Moreover, the maximum reflection loss and bandwidth corresponding to reflection loss below −10 dB of T-CNC material and plait-like CNCs are −36.09 and ca. −20 dB and 6.43 and 4.31 GHz, respectively. Thus, the T-CNC material is superior to plait-like CNCs in microwave absorption.

Acknowledgment. This work was financially supported by the Jiangsu Natural Science Foundation for Young Innovator (BK2007522), the National Natural Science Foundation (50602023), the National Major Project of Fundamental Research: Nanomaterials and Nanostructures (2005CB623605), P. R. China, and the National Science Council of Taiwan (NSC96-2627-M-005-001).

References and Notes

(1) Liu, Z.; Bai, G.; Huang, Y.; Li, F.; Ma, Y.; Guo, T.; He, X.; Lin, X.; Gao, H.; Chen, Y. *J. Phys. Chem. C* **2007**, *111*, 13696.

(2) Davis, W. R.; Slawson, R. J.; Rigby, G. R. *Nature* **1953**, *171*, 756.

(3) Iijima, S.; Ichihashi, T.; Ando, Y. *Nature* **1992**, *356*, 776.

(4) Amelinckx, S.; Zhang, X. B.; Bernaerts, D.; Zhang, X. F.; Ivanov, V.; Nagy, J. B. *Science* **1994**, *265*, 635.

(5) Akagi, K.; Tamura, R.; Tsukada, M.; Itoh, S.; Ihara, S. *Phys. Rev. Lett.* **1995**, *74*, 2307.

(6) Volodin, A.; Ahlskog, M.; Seynaeve, E.; Haesendonck, C. V.; Fonseca, A.; Nagy, J. B. *Phys. Rev. Lett.* **2000**, *84*, 3342.

(7) Hwang, W. I.; Chen, X. Q.; Kuzuya, T.; Kawabe, K.; Motojima, S. *Carbon* **2000**, *38*, 565.

(8) Kuzuya, C.; Kohda, M.; Hishikawa, Y.; Motojima, S. *Carbon* **2002**, *40*, 1991.

(9) Chen, X. Q.; Zhang, S. L.; Dikin, D. A.; Ding, W. Q.; Ruoff, R. S.; Pan, L. J.; Nakayama, Y. *Nano Lett.* **2003**, *3*, 1299.

(10) Fonseca, A. F. da; Galvão, D. S. *Phys. Rev. Lett.* **2004**, *92*, 175502.

(11) Bajpai, V.; Dai, L. M.; Ohashi, T. *J. Am. Chem. Soc.* **2004**, *126*, 5070.

(12) (a) Motojima, S.; Hoshiya, S.; Hishikawa, Y. *Carbon* **2003**, *41*, 2653. (b) Kajihara, Y.; Hihara, T.; Sumiyama, K.; Motojima, S. *Jpn. J. Appl. Phys.* **2005**, *44*, 6867. (c) Katsuno, T.; Chen, X. Q.; Yang, S. M.; Motojima, S.; Homma, M.; Maeno, T.; Konyo, M. *Appl. Phys. Lett.* **2006**, *88*, 232115. (d) Hayashida, T.; Pan, L.; Nakayama, Y. *Physica B* **2002**, *323*, 352.

(13) Pan, L.; Hayashida, T.; Zhang, M.; Nakayama, Y. *Jpn. J. Appl. Phys.* **2001**, *40*, 235.

(14) Motojima, S.; Hwang, W. I.; Kuzuya, T.; Iwanaga, H. *J. Mater. Sci.* **2001**, *36*, 71.

(15) Shibagaki, K.; Motojima, S. *Carbon* **2001**, *39*, 411.

(16) (a) Varadan, V. K.; Varadan, V. V. *Electromagnetic shielding and absorptive materials, U.S. Patent No. 89/03890*, 1989. (b) Neelakanta, P. S.; Subramaniam, K. *Adv. Mater. Processes* **1992**, *3*, 20. (c) Motojima, S.; Iwanaga, H.; Varadan, V. K. *Hyomen* **1998**, *36*, 140. (d) Chen, X. Q.; Motojima, S.; Iwanaga, H. *Carbon* **1999**, *37*, 1825. (e) Sun, G. S.; Yao, K. L.; Liao, H. X.; Niu, Z. C.; Liu, Z. L. *Int. J. Electron.* **2000**, *87*, 735. (f) Hishikawa, Y.; Kuzuya, C.; Hirako, S.; Hwang, W. I.; Motojima, S. *Trans. Mater. Res. Soc. Jpn.* **2002**, *27*, 39. (g) Kuzuya, C.; Motojima, S.; Kohda, M.; Hishikawa, Y. *Mater. Technol.* **2002**, *20*, 3. (h) Motojima, S.; Hoshiya, S.; Hishikawa, Y. *Carbon* **2003**, *41*, 2658. (i) Motojima, S.; Noda, Y.; Hoshiya, S.; Hishikawa, Y. *J. Appl. Phys.* **2003**, *94*, 2325. (j) Shen, Z. M.; Ge, M.; Zhao, D. L. *New Carbon Mater.* **2005**, *20*, 289. (k) Du, J. H.; Sun, C.; Bai, S.; Su, G.; Ying, Z.; Cheng, H. M. *J. Mater. Res.* **2002**, *17*, 1232.

(17) (a) Motojima, S.; Kawaguchi, M.; Nozaki, K.; Iwanaga, H. *Appl. Phys. Lett.* **1990**, *56*, 321. (b) Yang, S. M.; Hasegawa, M.; Chen, X. Q.; Motojima, S. *Carbon* **2007**, *45*, 1583. (c) Chen, X. Q.; Saito, T.; Kusunoki, M.; Motojima, S. *J. Mater. Res.* **1999**, *14*, 4329.

(18) Qin, Y.; Eggers, M.; Staedler, T.; Jiang, X. *Nanotechnology* **2007**, *18*, 345607.

(19) Tang, N. J.; Zhong, W.; Gedanken, A.; Du, Y. W. *J. Phys. Chem. B* **2006**, *110*, 11772.

(20) Tang, N. J.; Zhong, W.; Au, C. T.; Gedanken, A.; Yang, Y.; Du, Y. W. *Adv. Funct. Mater.* **2007**, *17*, 1542.

(21) Tang, N. J.; Yang, Y.; Lin, K. J.; Zhong, W.; Au, C. T.; Du, Y. W. *J. Phys. Chem. C* **2008**, *112*, 10061.

(22) Zhang, G. Y.; Jiang, X.; Wang, E. G. *Appl. Phys. Lett.* **2004**, *84*, 2646.

(23) Michielssen, E.; Sajer, J.; Ranjithan, S.; Mittra, R. *IEEE Trans. Microwave Theory Tech.* **1993**, *41*, 1024.

(24) (a) Che, R. C.; Peng, L. M.; Duan, X. F.; Chen, Q.; Liang, X. L. *Adv. Mater.* **2004**, *16*, 401. (b) Che, R. C.; Zhi, C. Y.; Liang, C. Y.; Zhou, X. G. *Appl. Phys. Lett.* **2006**, *88*, 033105. (c) Fan, Z. J.; Luo, G. H.; Zhang, Z. F.; Zhou, L.; Wei, F. *Mater. Sci. Eng., B* **2006**, *132*, 85.

(25) Zhu, H.; Lin, H. Y.; Guo, H. F.; Yu, L. F. *Mater. Sci. Eng., B* **2007**, *138*, 101.

(26) Yang, Y.; Zhang, B. S.; Xu, W. D.; Shi, Y. B.; Zhou, N. S.; Lu, H. X. *J. Alloys Comp.* **2004**, *365*, 300.

(27) Wu, M. Z.; He, H. H.; Zhao, Z. S.; Yao, X. *J. Phys. D: Appl. Phys.* **2000**, *33*, 2398.

(28) Zhang, X. F.; Dong, X. L.; Huang, H.; Liu, Y. Y.; Wang, W. N.; Zhu, X. G.; Lv, B.; Lei, J. P.; Lee, C. G. *Appl. Phys. Lett.* **2006**, *89*, 053115.

(29) Park, K. Y.; Lee, S. E.; Kim, C. G.; Han, J. H. *Compos. Sci. Technol.* **2006**, *66*, 576.

(30) Guire, T.; Varadan, V. V.; Varadan, V. K. *IEEE Trans. Electromagn. Compat.* **1990**, *32*, 300.

(31) Xie, G. W.; Wang, Z. B.; Cui, Z. L.; Shi, Y. L. *Carbon* **2005**, *43*, 3181.

(32) Fujii, M.; Matsui, M.; Motojima, S.; Hishikawa, Y. *J. Cryst. Growth* **2002**, *237*, 1937.

JP808087N